

Ternary Platinum-Multiwall Carbon Nanotube-Cobaltite Composites for Methanol Electrooxidation

R. Awasthi, R.N. Singh*

Chemistry Department, Centre of Advanced Study, Science Faculty, Banaras Hindu University, Varanasi-221005, India.

*E-mail: rnsbhu@rediffmail.com

Received: 25 March 2011 / Accepted: 2 September 2011 / Published: 1 October 2011

Ternary nanocomposite films of platinum, multiwall carbon nanotube (MWCNT) and cobaltite with composition 60wt%Pt-xwt%Co₃O₄-(40-x)wt%MWCNT (where x = 0, 5, 10, 20 and 25) are obtained on glassy carbon (GC) electrodes and investigated for electrocatalysis of the methanol oxidation reaction (MOR) in 0.5 M H₂SO₄. The study shows that introduction of 5 to 25wt%Co₃O₄ in place of MWCNT in the 60wt%Pt-40wt%MWCNT composite reduces the onset potential (E_{op}) and increases the rate of MOR significantly; the magnitudes of decrease in E_{op} and increase in the rate being the greatest with 10wt%Co₃O₄. The rate of MOR improved more than 50% with 10wt%Co₃O₄. The poisoning tolerance of the composite electrode was also observed to be better in presence of the oxide.

Keywords: Ternary composites, Methanol electrooxidation, Electrocatalysts, multiwall carbon nanotube, poisoning tolerance.

1. INTRODUCTION

The direct methanol fuel cells (DMFCs) have been documented as promising power sources for compact, high power density energy conversion [1,2]. Methanol is an efficient fuel and it can be obtained from natural gas, coal and biomass. Considerable interest has been devoted in recent years [3-14] to develop suitable electrode materials for the methanol oxidation reaction (MOR) for possible application in DMFCs. However, high overpotential for MOR prevents the use of DMFCs for practical purposes [3]. To reduce its overpotential, Pt and its alloys, particularly Pt-Ru, are considered as the best electrocatalysts [4]. But, during the electrooxidation of methanol, the intermediate, CO, is produced on the Pt electrode surface, which poisons the electrode surface [3]. To deal with the CO poisoning issue the most widely accepted strategy is to use suitable Pt based alloys [5-7] or Pt/metal

oxide composites [3,8-14]. The oxide is used to physically separate the catalytic particles and decrease their agglomeration rate thereby. Several oxides, such as WO_3 [3, 8], RuO_2 [9], SnO_2 [10], MnO_2 [11], CeO_2 [12], ZrO_2 [13] and MgO [14] have been reported to improve the electrocatalytic activity of Pt for the MOR.

Very recently, Singh and Awasthi [15], synthesized binary composites of Pt and multiwalled carbon nanotubes (MWCNTs) possessing 20, 40, 60, 70 and 80wt%Pt by the borohydride reduction method and investigated them as electrocatalysts for the MOR in 0.5 M H_2SO_4 . The Pt-40wt%MWCNT electrode of the investigation exhibited the highest catalytic efficiency for the MOR. To improve the efficiency of the catalyst further, we have now introduced Co_3O_4 nanopowder in place of MWCNT partially, keeping composition of Pt (60wt%) constant. The ternary composites, so derived, were 60wt%Pt-5wt% Co_3O_4 -35wt%MWCNT, 60wt%Pt-10wt% Co_3O_4 -30wt%MWCNT, 60wt%Pt-20wt% Co_3O_4 -20wt%MWCNT and 60wt%Pt-25wt% Co_3O_4 -15wt%MWCNT. The new composites have been observed to display considerably higher activity. Details of results of the MOR study on new composite electrodes in 0.5 M H_2SO_4 + 1 M CH_3OH are described in the present paper.

2. EXPERIMENTAL

2.1. Preparation of Composites

Nano-composites of Pt, MWCNT (Aldrich, Pr. No. 659258, dia. = 110-170 nm & length = 5-9 micron) and Co_3O_4 were obtained by NaBH_4 reduction method [15, 16]. For the purpose, the required amount of activated MWCNT (3-7 mg) and Co_3O_4 (1-5 mg) nanopowders were first dispersed in 2 ml double distilled water under ultrasonic stirring for 1 h and then required amounts of chloroplatinic acid (Aldrich, Pr.No.206083-1G) (31mg) was added and again ultrasonicated for 1 h. To this, an excess of NaBH_4 (Sigma–Aldrich, Pr .No.452874) solution was added under vigorous stirred condition to carry out the complete reduction of metal ions. For addition of the Pt precursor salt, a stock solution of chloroplatinic acid in acidified double distilled water (20 mg ml^{-1}) was used. After completion of the reduction process, the product was separated through centrifugation, repeatedly washed with double distilled water so as to remove Cl^- ions and finally dried overnight in a vacuum oven at 373 K. Thus, the desired 60wt%Pt-xwt% Co_3O_4 -(40-x)wt% MWCNT ($x = 0, 5, 10, 20$ and 25) composites were obtained. As mentioned earlier [16,17], the activation of MWCNT was carried out by refluxing it in concentrated HNO_3 for 5 h. Cobaltite (Co_3O_4) was prepared by the hydroxide carbonate co-precipitation method as described elsewhere [18].

2.2. Preparation of electrodes

The catalyst (composite) was dispersed in a ternary mixture of double distilled water, isopropanol and ethanol (1:1:2). The mixture was then sonicated to get a homogenous suspension. It was then dropped (2-3 drops) on a pretreated glassy carbon (GC) plate through a syringe and dried. Finally, one drop of 1wt% Nafion solution (Alfa Aesar) was dropped over the dried catalyst layer so as

to enhance the adherence of the catalytic film. Prior to use the GC electrode as support for the catalyst over layer, it was polished well on a polishing machine using a microcloth pad and alumina powder, dipped in 0.2 M H_3PO_4 for 5 min, degreased in acetone for 4 min ultrasonically, washed with double distilled water and then dried. The electrodes, thus obtained, were finally irradiated with microwave (800 Watt) for 1 min. Electrical contact with the catalyst film was made as described elsewhere [19].

2.3. Material Characterization

X-ray diffraction (XRD) patterns of the composite films as- obtained on GC were recorded by an X-ray diffractometer (Thermo Electron) at a sweep rate of 3° min^{-1} using Cu K_α as the radiation source ($\lambda = 1.541841 \text{ \AA}$). Morphology of the catalytic films was studied by a transmission electron microscope (TECNAIG² FEI Neederland). Samples for TEM analyses were prepared by dispersing the catalyst into methanol, transferring a drop of this suspension onto a carbon coated copper grid, and subsequently drying in air.

2.4. Electrochemical study

Electrochemical studies were carried out in a conventional three-electrode single compartment Pyrex glass cell. The potential of the working electrode was measured against the SCE electrode (0.242 V vs. S H E). The counter electrode was a Pt plate with a geometrical area of $\sim 8 \text{ cm}^2$. The potential values mentioned in the text are referred against the SCE electrode only. Electrochemical studies, namely, cyclic voltammetry (CV) and chronoamperometry have been carried out by a computer controlled EG & G PAR potentiostat /galvanostat (Model: 273A).

CV of each electrocatalyst was recorded in 0.5 M H_2SO_4 with and without containing 1 M CH_3OH at 298 K. Before recording the final voltammogram, each electrode was cycled for five runs at a scan rate of 50 mV s^{-1} in the electrolyte. All electrochemical experiments were performed in an Ar-deoxygenated electrolyte at 298 K. The mass of the catalytic films on GC was 0.2-0.3 mg cm^{-2} and the geometrical area of each catalyst electrode was close to 0.5 (i.e., 0.48-0.52) cm^2 .

3. RESULTS AND DISCUSSION

3.1. X-ray diffraction (XRD)

XRD patterns of composites, Pt-40wt%MWCNT, Pt-5wt% Co_3O_4 -35wt%MWCNT, Pt-10wt% Co_3O_4 -30wt%MWCNT, and Pt-25wt% Co_3O_4 -15wt%MWCNT are shown in Fig.1. The XRD pattern of each catalyst exhibits the face centered cubic (fcc) crystal structure and the diffraction peaks at the Bragg angles of 40° , 46.07° and 67.28° correspond to planes (111), (200) and (220) of Pt (JCPDS 04-0802). Thus, result shows that Pt exists in the metallic phase in the composites. The observed diffraction peaks at $2\theta \approx 36.45$, 55.46 , 59.24 and 65.1° correspond to the spinel Co_3O_4

(JCPDS 09-0418). The intense Pt (111) diffraction peak was used to estimate the crystallite size of Pt in the composite using Scherrer formula.

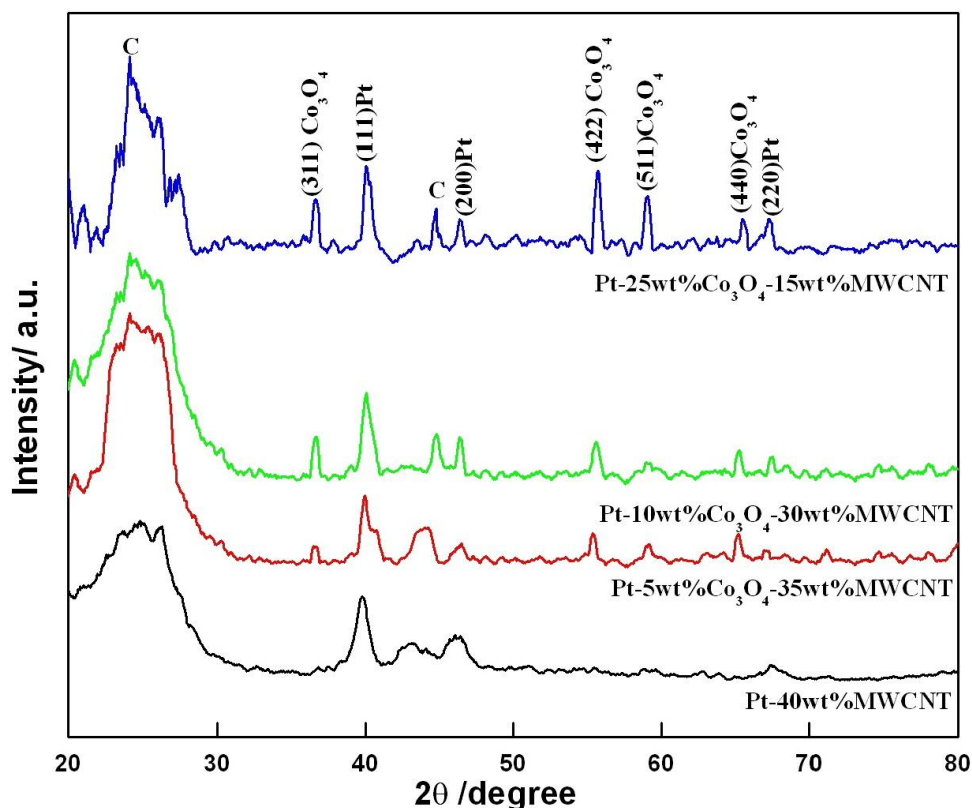


Figure1. XRD patterns of: Pt-40wt%MWCNT, Pt-5wt%Co₃O₄-35wt%MWCNT, Pt-10wt%Co₃O₄-30wt%MWCNT and Pt-25wt%Co₃O₄-15wt%MWCNT as deposited on GC.

Estimates of crystalline size of Pt were found to be 10.8, 10.8, 9.3 and 15.3 nm in Pt-40wt%MWCNT, Pt-5wt%Co₃O₄-35wt%MWCNT, Pt-10wt%Co₃O₄-30wt%MWCNT and Pt-25wt%Co₃O₄-15wt%MWCNT, respectively. This result shows that 5 to 10 wt% oxide additions do not influence the particle size of Pt practically, however, its higher addition (25wt%) seems to influence.

3.2. TEM analysis

Fig.2 shows TEM images of Pt-xwt%Co₃O₄-(40-x)wt%MWCNT- (where x = 0, 5, 10 and 25). Fig.2 (a-c) shows that the dispersion of Pt particles are better in the case of catalyst with 5wt%Co₃O₄. Metal nanoparticles seem to be more populated in the region of joints and defects of MWCNTs (Fig.2b). The formation of some agglomerates also takes place on the MWCNT surface. These agglomerates are, in fact, formed with spherical nanoparticles of Pt.

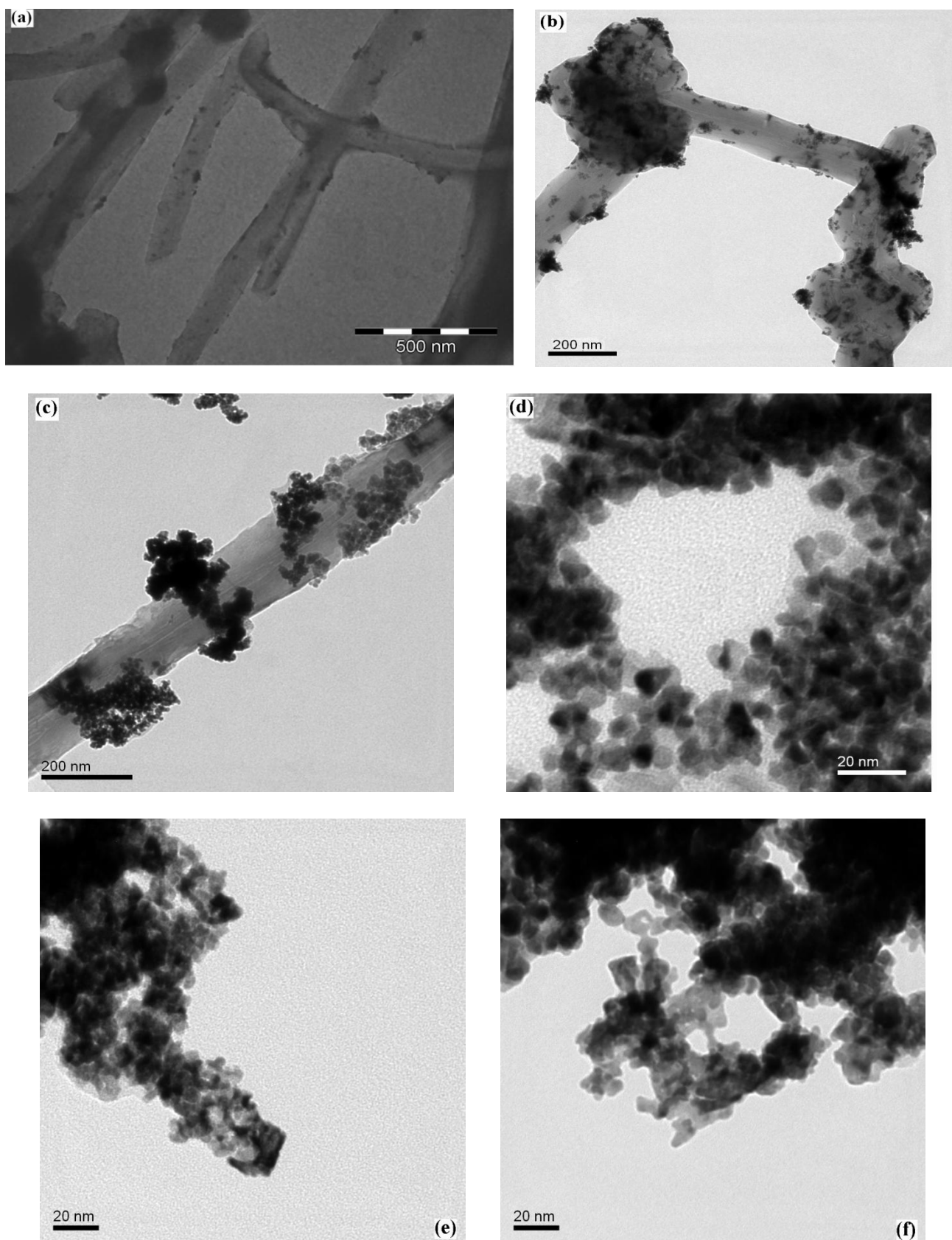


Figure 2. TEM images of (a) Pt-40wt%MWCNT (500 nm), (b) Pt-5wt% Co_3O_4 -35wt%MWCNT (200 nm), (c) Pt-10wt% Co_3O_4 -30wt%MWCNT (200 nm), (d) Pt-5wt% Co_3O_4 -35wt%MWCNT (20 nm), (e) Pt-10wt% Co_3O_4 -30wt%MWCNT (20 nm) (f) Pt-25wt% Co_3O_4 -15wt%MWCNT (20 nm), respectively.

The particle size of active component (Pt) ranged between 7 and 10 nm, 6 and 9 nm, and 12 and 16 nm in the composites containing 5, 10 and 25wt% Co_3O_4 , respectively. These results were found to be similar to those obtained from XRD data.

The observation of Fig.2 (d-f) indicates that nanoparticles attached to the surface of MWCNTs are coated with a thin layer, essentially of Co_3O_4 . Some dendritic growth of metal nanoparticles was also found as is quite apparent in the case of the catalyst with 10wt% Co_3O_4 (Fig.2c).

3.3. Cyclic voltammetry (CV)

CVs of Pt-40wt%MWCNT, Pt-5wt% Co_3O_4 -35wt%MWCNT, Pt-10wt% Co_3O_4 -30wt%MWCNT, Pt-20wt% Co_3O_4 -20wt%MWCNT and Pt-25wt% Co_3O_4 -15wt%MWCNT were recorded at the scan rate of 50 mV s^{-1} at 298 K and curves, so obtained, are reproduced in Fig.3 and 4.

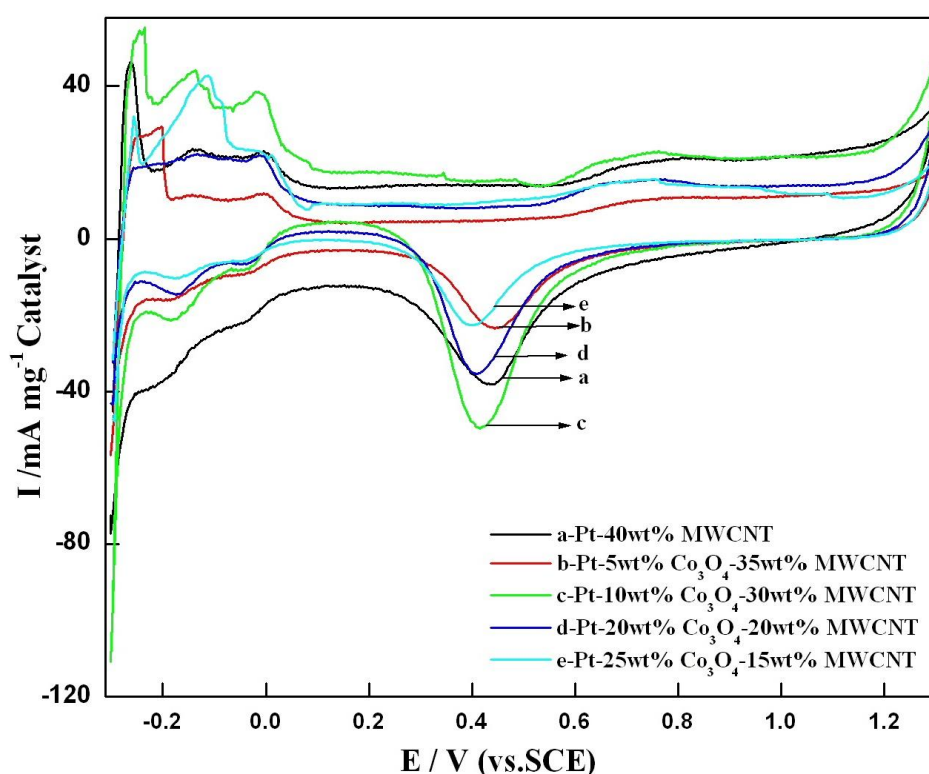


Figure 3. Cyclic voltammograms of Pt-xwt% Co_3O_4 -(40-x)wt%MWCNT ($x = 0, 5, 10, 20$ and 25) composites at a scan rate of 50 mV s^{-1} in $0.5 \text{ M H}_2\text{SO}_4$ at 298 K.

The electrolytes used were $0.5 \text{ M H}_2\text{SO}_4$ and $1 \text{ M CH}_3\text{OH} + 0.5 \text{ M H}_2\text{SO}_4$. Fig.3 gathers CV curves for composite electrodes in $0.5 \text{ M H}_2\text{SO}_4$ (without containing methanol) in the potential range of -0.3 to $+1.3 \text{ V}$. Features of CV curves were almost similar. Similar voltammograms were also obtained on $\text{Co}_3\text{O}_4/\text{Pt}$ nanocomposite in $0.5 \text{ M H}_2\text{SO}_4$ [20]. These CV curves demonstrate two cathodic and two to three anodic peaks between -0.3 V and $+0.1 \text{ V}$. These are characteristic peaks for the

adsorption and desorption of Hydrogen atom [21]. The difference in the CV Profile can be ascribed to a change in the surface crystallinity [15, 21]. The strong cathodic peak at $E = \sim 0.40$ V is produced due to reduction of Pt (II) into Pt (0) [15, 22]. A broad anodic peak, in the potential range, 0.60 V- 0.90 V, observed well before the oxygen evolution peak (1.2-1.3 V), corresponds to the oxidation of Pt metal into PtO [15, 21].

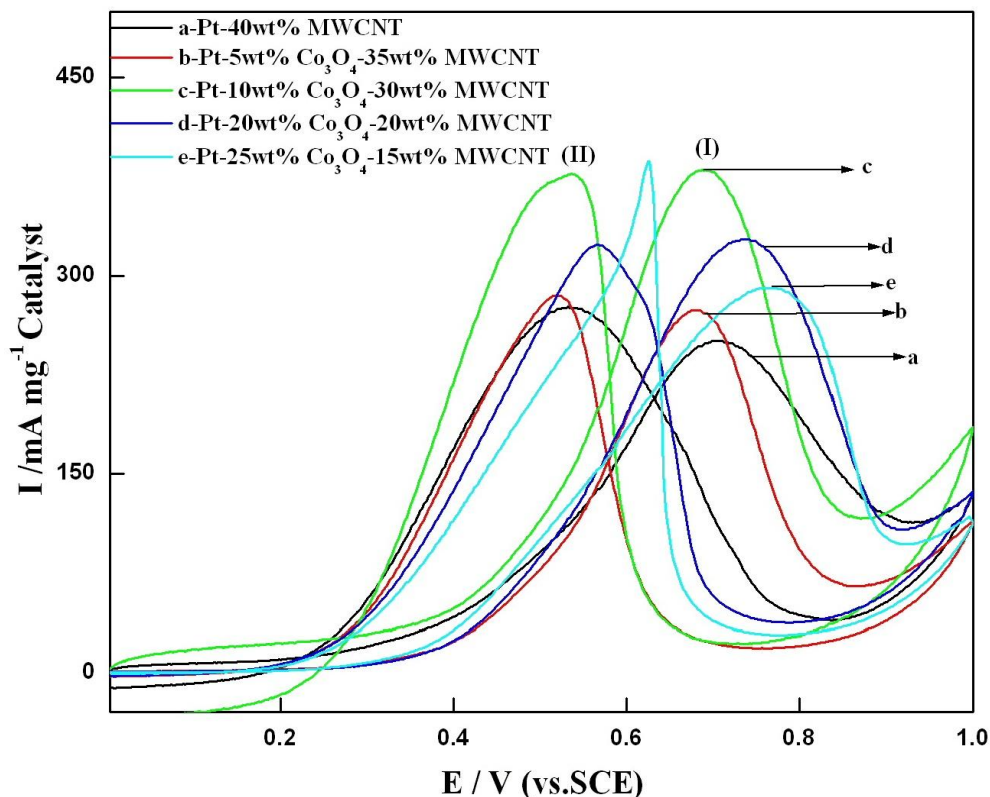


Figure 4. Cyclic voltammograms of Pt-xwt%Co₃O₄-(40-x)wt%MWCNT ($x = 0, 5, 10, 20$ and 25) composites at a scan rate of 50 mV s^{-1} in $0.5 \text{ M H}_2\text{SO}_4 + 1 \text{ M CH}_3\text{OH}$ at 298 K .

Table 1. Results of cyclic voltammetry of Pt-xwt%Co₃O₄-(40-x)wt%MWCNT composite electrodes in $0.5 \text{ M H}_2\text{SO}_4 + 1 \text{ M CH}_3\text{OH}$ at 298 K .

x	EASA ($\text{cm}^2 \text{ mg}^{-1} \text{ Pt}$)	E_{op} (mV)	E_{p} (mV)	I_{p} ($\text{mA mg}^{-1} \text{ catalyst}$)	I ($\text{mA mg}^{-1} \text{ catalyst}$) at $E = 0.65 \text{ V}$	SA (mA cm^{-2})
0	506 ± 5	261 ± 2	712 ± 7	245 ± 6	225 ± 8	0.7 ± 0.1
5	440 ± 5	166 ± 8	681 ± 4	272 ± 2	259 ± 3	1.0 ± 0.1
10	463 ± 12	71 ± 2	688 ± 1	399 ± 19	353 ± 14	1.3 ± 0.1
20	419 ± 17	131 ± 25	751 ± 9	331 ± 3	264 ± 6	1.0 ± 0.1
25	390 ± 6	166 ± 18	773 ± 5	285 ± 3	228 ± 2	1.0 ± 0.1

Fig.4 gathers cyclic voltammograms for Pt -xwt%Co₃O₄-(40-x)wt%MWCNT (x = 0, 5, 10, 20 and 25) electrodes in the potential range, 0.0 - 1.0 V in 0.5 M H₂SO₄+1 M CH₃OH. CV curves, so obtained were more or less similar and are given in Fig.4. This figure displays two well defined anodic current peaks, one in the forward (I) (i.e. under anodic condition) and the other one (II) in the reverse (i.e. under cathodic condition) scan. The two anodic current peaks are the characteristics of the MOR and have been observed in case of methanol electrooxidation on all Pt and Pt alloys/composites reported in literature [15, 21, 23-25]. CV curves of Fig. 4 were analyzed for the onset potential (E_{op}), peak current (I_p) and peak potential (E_p) and values are listed in Table1.

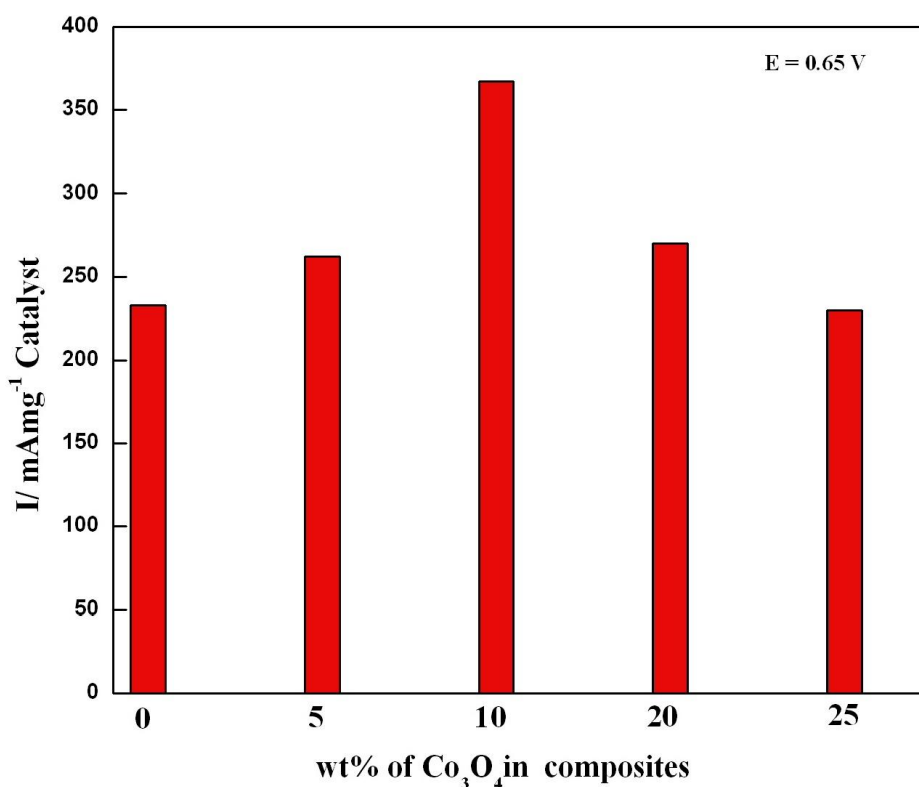


Figure 5. Bar diagram: the catalytic activity of the composite as a function of composition of the oxide at E = 0.65 V in 0.5 M H₂SO₄+ 1 M CH₃OH at 298 K.

The onset potential for the MOR is a determining element in evaluating the activity of an electrode. From Table1, it is clear that presence of the metal oxide from 5 to 25wt% in the composite electrode shifts the onset potential towards less positive direction, the magnitude of the shift being the largest with 10wt%Co₃O₄. Thus, the catalytic activity of the composite electrode seems to be promoted in presence of Co₃O₄. The mass activity, i.e. the peak current normalized to mass of catalyst loading (I_p), determined from Fig.4 (Table1) also shows an increase with the Co₃O₄-content, the best performance, however, being found with 10wt% Co₃O₄ in the ternary composite.

Results shown in Table1 and Fig.4 show that the peak potential for the MOR varies with the nature of electrocatalyst. So, for making a real comparison the electrocatalytic activities of Pt-MWCNT-Co₃O₄ composite electrodes have been determined at a common and constant potential,

chosen prior to the methanol oxidation peak current on the forward scan, from Fig.4 and expressed as a function of wt% of Co_3O_4 in the composite catalyst as shown in Fig.5. This figure clearly demonstrates that the rate of methanol oxidation is the highest with 10wt% Co_3O_4 . So, the Pt-10wt% Co_3O_4 -30wt%MWCNT electrode is the best electrocatalyst of the present investigation.

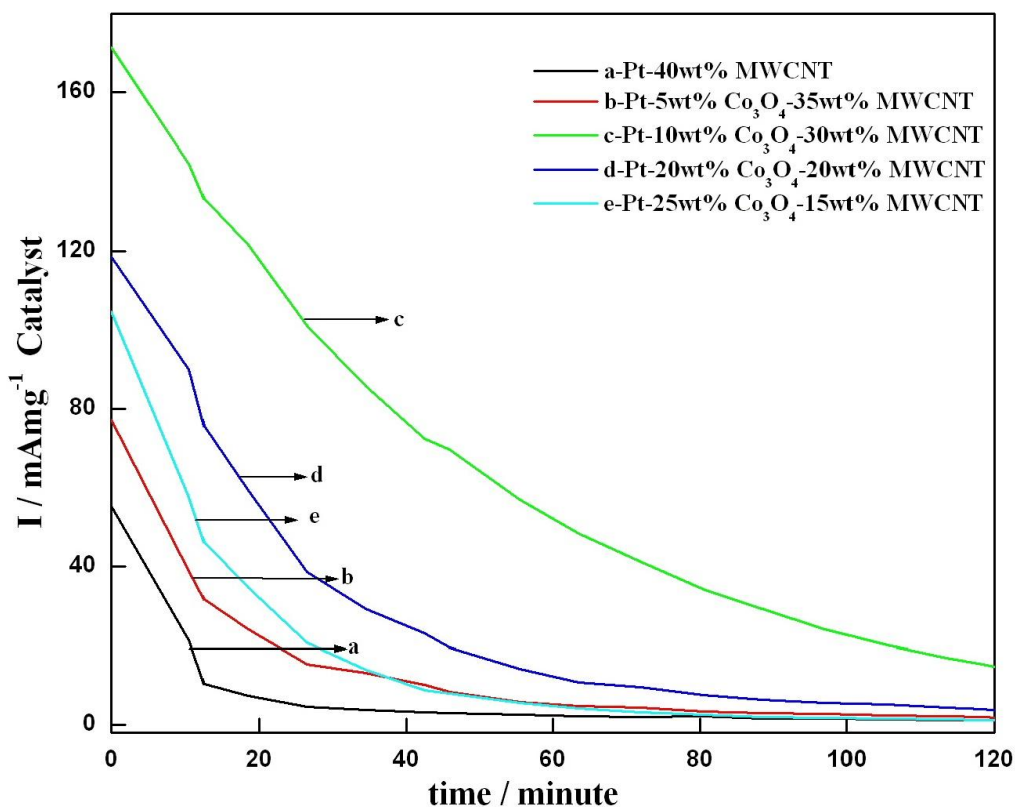


Figure 6. Stability curves for Pt-xwt% Co_3O_4 -(40-x)wt%MWCNT ($x = 0, 5, 10, 20$ and 25) composites in $0.5 \text{ M H}_2\text{SO}_4 + 1 \text{ M CH}_3\text{OH}$ at $E = 0.60 \text{ V}$.

In order to understand the role of Co_3O_4 in electrocatalysis of the MOR, the electrochemical active surface areas (EASAs) of the composite electrodes have also been determined by measuring the coulombic charge (Q_H) required for the electrochemical adsorption of hydrogen atom on Pt, details of which are given elsewhere [15,26]. For the purpose, the two cathodic peaks, observed between -0.3 and $+0.10 \text{ V}$, in the cyclic voltammogram of the compound, which correspond to the electro-adsorption of the hydrogen atom on to the metallic Pt surface, have been employed for the estimation of EASA using the relation [15,27,28],

$$EASA = \frac{Q_H}{Q_{H,ref}}$$

where Q_H is the amount of charge exchanged during the electro-sorption of hydrogen atoms onto the Pt surface and $Q_{H,ref}$ is considered to be 0.21 mC cm^{-2} in the case of Pt. This value corresponds to a surface density of $1.3 \times 10^{15} \text{ atom / cm}^2$, a generally accepted value for polycrystalline Pt electrode [15, 29]. Q_H was determined by integrating the area under the cathodic curves, observed between -0.3 and $+0.10 \text{ V}$, through an integrator facility provided in the instrument (potentiostat /galvanostat). Estimates of EASA of electrodes are shown in Table1.

From Table1 it is clear that replacement of 5 to 25wt% MWCNT by Co_3O_4 in the Pt-40wt% MWCNT composite seems to slightly decrease the EASA, nevertheless, the methanol oxidation current increases significantly. This result demonstrates that addition of the oxide somewhat influences the electronic properties of the material, which is quite evident from Table1 wherein the Specific activity ($SA = I, \text{ mA mg}^{-1}_{Pt} / \text{EASA, cm}^2 \text{ mg}^{-1}_{Pt}$) of Co_3O_4 substituted products are 1.5 - 1.8 times higher than the base, Pt-40wt%MWCNT electrode. Thus, the role of the cobalt oxide seems to weaken the bond between CO and Pt, which originates in the modification of electronic band structure of Pt and interaction between Pt and the oxide. Further, Co_3O_4 is known [30] to possess surface adsorbed oxygen species which might also enhance the oxidation of CO to CO_2 . The observation of TEM picture indicates that elemental Pt preferably gets adsorbed on the MWCNT surface due to presence of several functional groups such as hydroxyl, carboxylic acid and carbonyl [15], and that the Co_3O_4 nanoparticles appears to present on the surface of adsorbed Pt metal as an over layer. The thickness of the overlayer somewhat increases with an increase in weight percentage of Co_3O_4 (Fig.2 d-f). The cobalt oxide being a semiconductor [31] might influence the resistivity of the catalyst layer and hence the electrocatalytic activity, particularly at its higher addition.

3.4. Chronoamperometry

Fig.6 gathers chronoamperograms of the catalysts Pt-xwt% Co_3O_4 (40-x)wt%MWCNT ($x = 0, 5, 10, 20$ and 25) at $E = 0.60 \text{ V}$ in $0.5 \text{ M H}_2\text{SO}_4 + 1 \text{ M CH}_3\text{OH}$. Curves shown in Fig.6 demonstrates that the composite electrodes containing 10wt% oxide has considerably improved performance as well as poisoning tolerance compared to the Pt-40wt%MWCNT electrode. This is quite evident from values of the current observed at 60 min during the experiment, which were $\sim 51 \text{ mA mg}^{-1}$ and 3 mA mg^{-1} on Pt-10wt% Co_3O_4 -30wt%MWCNT and Pt-40wt%MWCNT, respectively.

4. CONCLUSIONS

The study has indicated that addition of the cobaltite nanoparticles from 5 to 25wt% for MWCNTs in the 60wt%Pt-40wt%MWCNT nanocomposite slightly decreases the electrochemical surface area but, on contrary, it improves both the apparent as well as the specific (true) catalytic activity considerably. The increase in catalytic activity with cobaltite addition has been ascribed to the modification in the electronic properties of the composite material in favor of electrocatalysis of MOR, improvement, however, being the greatest in the case of 10wt% Co_3O_4 . The poisoning tolerance of the

composite electrode containing 10wt%Co₃O₄ was also the greatest during electrolysis in 0.5 M H₂SO₄ + 1 M CH₃OH. Presence of Co₃O₄ in the Pt – MWCNT composite is considered to modify the electronic band structure of Pt and interaction between Pt and the oxide resulting in weakening the bond between CO and Pt.

ACKNOWLEDGMENTS

One of authors (RA) thanks the Council of Scientific and Industrial Research (CSIR) New Delhi for the award of the Senior Research Fellowship to carry out the investigation. We also thank Prof. Gouthama, Department of Material and Metallurgical Engineering, I.I.T. Kanpur for TEM analysis.

References

1. G. Q. Lu, C. Y. Wang, T. J. Yen and X. Zhang, *Electrochim. Acta*, 49 (2004) 821.
2. G. Q. Lu and C. Y. Wang, *J. Power Sources*, 144 (2005) 141.
3. B. Rajesh, V. Karthik, S. Karthikeyan, K. R. Thampi, J. M. Bonard and B. Viswanathan, *Fuel*, 81 (2002) 2177.
4. J. Guo, G. Sun, Q. Wang, G. Wang, Z. Zhou, S. Tang, L. Jiang, B. Zhou and Q. Xin, *Carbon*, 44 (2006) 152.
5. L. Jiang, G. Sun, S. Sun, J. Liu, S. Tang, H. Li, B. Zhou and Q. Xin, *Electrochim. Acta*, 50 (2005) 5384.
6. K. B. Kokoh, F. Hahn, E. M. Belgsir, C. Lamy, A. R. deAndrade, P. Olivi, A. J. Motheo and G. T. Filho, *Electrochim. Acta*, 49 (2004) 2077.
7. B. N. Grgur, N. M. Markovic and P. N. Ross, *Electrochim. Acta*, 43 (1998) 3631.
8. V. Raghuvver and B. Viswanathan, *J. Power Sources*, 144 (2005) 1.
9. H. B. Suffredini, V. Tricoli, L. A. Avaca and N. Vatistas, *Electrochem. Commun.*, 6 (2004) 1025.
10. A. L. Santos, D. Profeti and P. Olivi, *Electrochim. Acta*, 50 (2005) 2615.
11. G.-Y. Zhao and H.-L. Li, *Appl. Surf. Sci.*, 254 (2008) 3232.
12. C. Xu and P. K. Shen, *Chem. Commun.*, 19 (2004) 2238.
13. Y. Bai, J. Wu, J. Xi, J. Wang, W. Zhu, L. Chen and X. Qiu, *Electrochem. Commun.*, 7 (2005) 1087.
14. C. Xu, P. K. Shen, X. Ji, R. Zeng and Y. Liu, *Electrochem. Commun.*, 7 (2005) 1305.
15. R. N. Singh and R. Awasthi, *The Open Catalysis Journal*, 3 (2010) 54.
16. R. N. Singh, A. Singh and Anindita, *Carbon*, 47 (2009) 271.
17. J. Wang, J. Xi, Y. Bai, Y. Shen, J. Sun, L. Chen, W. Zhu and X. Qiu, *J. Power Sources*, 164 (2007) 555.
18. B. Lal, N. K. Singh, S. Samuel and R. N. Singh, *J. New Mater. Electrochem. Systems*, 2 (1999) 59.
19. R. N. Singh, T. Sharma, A. Singh, Anindita, D. Mishra and S. K. Tiwari, *Electrochim. Acta*, 53 (2008) 2322.
20. H. J. Ahn and T. Y. Seong, *J. Alloys and Compounds*, 478 (2009) L8.
21. M. Umeda, M. Kokubo, M. Mohamedi and I. Uchida, *Electrochim. Acta*, 48 (2003) 1367.
22. M. K. Jeon, Y. Zhang and P. J. McGinn, *Electrochim. Acta*, 54 (2009) 2837.
23. C. T. Hsieh and J. Y. Lin, *J. Power Sources*, 188 (2009) 347.
24. Y. Liang, J. Li, Q. C. Xu, R. Z. Hu, J. D. Lin and D. W. Liao, *J. Alloys and compounds*, 465 (2008) 296.
25. P. K. Shen and Z. Tian, *Electrochim. Acta*, 49 (2004) 3107.
26. B. Xu, J. Guo, H. Jia, X. Yang and X. Liu, *Catalysis Today*, 125 (2007) 169.
27. M. Watanabe, K. Makita, H. Usami and S. Motoo, *J. Electroanal. Chem.*, 197 (1986) 195.
28. Y.C. Liu, X. P. Qiu, Y. Q. Huang and W. T. Zhu, *Carbon*, 40 (2002) 2375.

29. G. Faubert, D. Guay and J. P. Dodelet, *J. Electrochem. Soc.*, 145 (1998) 2985.
30. Y. Xia, H. Dai, H. Jiang and L. Zhang, *Catalysis Commun.*, 11 (2010) 1171.
31. C. Xu, Z. Tian, P. Shen and S. P. Jiang, *Electrochim. Acta*, 53 (2008) 2610.